photonics

MDPI

Article

Twisted Multi-Cosine Gaussian Schell-Model Arrays and Their Statistical Characteristics

Miaomiao Tang *, Shijie Dong, Pengju Yuan, Yunzhe Yang, Yujie Zhou and Xinzhong Li

School of Physics and Engineering, Henan University of Science and Technology, Luoyang 471023, China
* Correspondence: tmiaomiao0371@163.com

Abstract: A novel class of random sources with a twisted multi-cosine Gaussian Schell model correlation function is introduced, termed the TMCGSM array. The spectral density and spectral degree of coherence of the TMCGSM array field upon propagation are investigated thoroughly. Numerical examples illustrate that such beams are capable of producing a non-uniform lattice profile in the far zone and exhibits an unusual rotation behavior. It is revealed that the twist factor can not only induce the array to rotate as a whole, but also has a modulation effect on the intensity of element lobes in the central area. We also demonstrated that an obvious twist effect could be observed in the coherence curves under certain conditions.

Keywords: twisted partially coherent beam; coherence structure; array beams; propagation

1. Introduction

There has been a wealth of interests in developing new classes of partial coherent wavefields due to their significant merits in applications such as optical communication, atomic cooling, encryption and target detection [1–8]. As a celebrated example, Simon and Mukunda proposed the twisted Gaussian Schell-model (TGSM) 30 years ago, by introducing a twist phase into the cross-spectral density (CSD) of a Gaussian Schell-model source [9]. A twist phase is a non-separable statistical phase between two spatial points, as demonstrated in $\exp[iu(x_1y_2 - x_2y_1)]$ with u being the twist factor. The nonlocal term gives the beam field a definite handedness and allows the intensity spot to rotate along the propagation axis. It is worth noting that a twist phase can only survive in partially coherent beams. Since then, much research has examined the striking features of TGSM optical fields in free space and in various kinds of media [9–15]. Undoubtedly, the twist phase has been regarded as an important modulation dimension in the area of low coherent optical beams.

Most literatures involving twisted fields are restricted to the original model presented in [2]; however, it is tricky to introduce twisted CSDs of non-Gaussian forms. The difficulty lies in the physical realizability of twisted CSDs. More precisely, one cannot stick a twist term to a valid CSD at will, because it may violate the constraint of non-negative definiteness. Until recently, promising progress has been made in the devising of twisted nontrivial correlated fields. For example, Borghi discussed whether a twist can be added on a Schell-model correlated beam [16]. Gori and Santarsiero proposed a new approach to construct genuine twisted CSDs without symmetry requirements [17]. Mei and Korotkova established an effective procedure to design novel twisted sources by using the modal representation method [18]; they also illustrated the propagating properties of EM twisted beams with structured correlation [19]. Cai et al. experimentally synthesized anisotropic TGSM beams using discrete model sampling [20], and realized the generation of twisted correlated beams with a single spatial light modulator [21]. Zhou et al. discussed the effect of the twist phase on radially polarized partially coherent beams and demonstrated that the existence of the twist phase is a double-edged sword for the self-healing properties of the beam [22]. Yang et al. proposed a class of twisted circle Pierce vortex beams and then

check for updates

Citation: Tang, M.; Dong, S.; Yuan, P.; Yang, Y.; Zhou, Y.; Li, X. Twisted Multi-Cosine Gaussian Schell-Model Arrays and Their Statistical Characteristics. *Photonics* **2024**, *11*, 1139. https://doi.org/10.3390/photonics11121139

Received: 13 November 2024
Revised: 30 November 2024
Accepted: 2 December 2024
Published: 4 December 2024

Copyright: © 2024 by the authors. Licensee MDPI, Basel, Switzerland. This article is an open access article distributed under the terms and conditions of the Creative Commons Attribution (CC BY) license (https://creativecommons.org/licenses/by/4.0/).

verified that such beams have a great advantage in localized particle capture and particle rotation [23]. Fu et al. generated a hollow twisted correlated beam which showed an asymmetric orbital angular momentum spectral distribution and a tunable intensity center [24]. Very recently, Qian et al. introduced a general approach to generate twisted structured beams by superposing the spiral sub-phase with different azimuthal rotation factors [25]. These studies have provided a broader basis for research involving the twist effect.

Spatial lattices fields have a broad range of applications in optical sensing, trapping cold atoms, and other fields [26–28]. Due to this potential, much effort has been paid to design optical lattices with various profiles, such as Gaussian Schell-model arrays (GSMA) [29], optical coherence lattices [30], ring-shaped lattice beams [31], and rectangular optical arrays [32]. In recent years, the possibility of endowing a twist to arrays has been achieved, and different kinds of sources for generating twisting lattice-like intensity distribution have been proposed [33–37]. For example, Zhao et al. proposed a class of twisted GSMA beams by mapping the twist phase to the CSD of GSMA [33]. The effect of random turbulence on the statistical properties of twisted GSMA have been discussed [34,35]. Wang et al. devised a twisted random field with a ring-shaped array profile [36]. However, almost all of these examples were generated by sticking a twist term to non-CSDs, which reveals that they show lattice distributions with identical element lobes and present the same rotation mode. Thus, it is highly desirable to introduce partially coherent array fields with non-trivial twist features. In this manuscript, we introduce a new kind of twisted array field termed the twisted multi-cosine Gaussian Schell-model (TMCGSM) array field. Such a field is characterized by its non-uniform lattice distribution and unfamiliar rotation mode. The spectral density and spectral degree of coherence of the field upon propagation could be properly controlled by the twist factor and coherence parameters of the source.

2. Analytic Solutions for Twisted Multi-Cosine Gaussian Schell-Model Arrays

Consider an optical field generated by a random, statistically stationary source located in the plane $z = 0$. The spectral spatial coherent properties of the beam at a pair of points $\boldsymbol{\rho}_1' = (x_1', y_1')$ and $\boldsymbol{\rho}_2' = (x_2', y_2')$ are represented by the CSD function [1]:

$$W^{(0)}(\boldsymbol{\rho}_1', \boldsymbol{\rho}_2', \omega) = \left\langle E^*(\boldsymbol{\rho}_1', \omega) E(\boldsymbol{\rho}_2', \omega) \right\rangle, \tag{1}$$

where $E(\boldsymbol{\rho}', \omega)$ represents the electric field. The asterisk and angle brackets denote the complex conjugate and ensemble average, respectively. As we know, a physically realized partially coherent source suffices when written in a superposition integral form [38]

$$W^{(0)}(\boldsymbol{\rho}_1', \boldsymbol{\rho}_2') = \iint p(\boldsymbol{v}) H^*(\boldsymbol{\rho}_1', \boldsymbol{v}) H(\boldsymbol{\rho}_2', \boldsymbol{v}) \mathrm{d}^2\boldsymbol{v}, \tag{2}$$

where H is an arbitrary kernel, and $p(\boldsymbol{v})$ denotes a weight function which decides the correlation type.

To generate a twisted field, one may select the kernel as:

$$H(\boldsymbol{\rho}', \boldsymbol{v}) = \tau(\boldsymbol{\rho}') \exp[-(uy' + ix')v_x + (ux' - iy')v_y], \tag{3}$$

where $\tau(\boldsymbol{\rho}')$ denotes an amplitude function, and u represents the twist factor.

We select the weight function to take the following form [29]:

$$\begin{aligned} p(\boldsymbol{v}) = \; & \frac{2\pi\delta_x\delta_y}{NM} \exp\left[-2\pi^2\left(\delta_x^2 v_x^2 + \delta_y^2 v_y^2\right)\right] \\ & \times \sum_{n=-P}^{P} \cosh\left(4\pi^2\delta_x n R_x v_x\right) \exp\left(-2\pi^2 n^2 R_x^2\right) \\ & \times \sum_{m=-Q}^{Q} \cosh\left(4\pi^2\delta_y m R_y v_y\right) \exp\left(-2\pi^2 m^2 R_y^2\right), \end{aligned} \tag{4}$$

with $\cosh(x)$ being the hyperbolic cosine function. δ_i and $R_i (i = x, y)$ are positive real constants, $P = (N-1)/2$ and $Q = (M-1)/2$.

Further, we select the Gaussian profile for function $\tau(\boldsymbol{\rho}')$, which can be given by

$$\tau(\boldsymbol{\rho}') = \exp\left(-\frac{x'^2}{2\sigma_x^2}\right)\exp\left(-\frac{y'^2}{2\sigma_y^2}\right), \tag{5}$$

where σ_x and σ_y denote source widths.

By substituting Equations (3)–(5) into Equation (2), we obtain the CSD function of a TMCGSM array in the source plane as follows:

$$\begin{aligned} W^{(0)}(\rho_1', \rho_2') = \; & \frac{1}{MN}\exp\left(-\frac{x_1'^2 + x_2'^2}{2\sigma_x^2} - \frac{y_1'^2 + y_2'^2}{2\sigma_y^2}\right) \\ & \times \exp\left[-\frac{(x_1' - x_2')^2 - u^2(x_1' + x_2')^2}{2\delta_x'^2} - \frac{(y_1' - y_2')^2 - u^2(y_1' + y_2')^2}{2\delta_y'^2}\right] \\ & \times \exp\left[-\frac{iu(y_1' + y_2')(x_1' - x_2')^2}{\delta_x'^2} + \frac{iu(x_1' + x_2')(y_1' - y_2')}{\delta_y'^2}\right] \\ & \times \sum_{n=-P}^{P} \cos\left\{\frac{2\pi n R_x}{\delta_x'}\left[-iu(y_1' + y_2') - (x_1' - x_2')\right]\right\} \\ & \times \sum_{m=-Q}^{Q} \cos\left\{\frac{2\pi m R_y}{\delta_y'}\left[-iu(x_1' + x_2') - (y_1' - y_2')\right]\right\}, \end{aligned} \tag{6}$$

with $\delta_x' = 2\pi\delta_x$ and $\delta_y' = 2\pi\delta_y$. It is seen that the field reduces to a GSMA with the choice of $u = 0$. Notably, the twist term does not perform as a twist phase, but exists in the multi-cosine correlation function, which is quite distinct from the twisted GSMA beam presented in [33]. Thus, an interesting twist effect can be expected for the new twisted source.

Suppose that this novel beam passes through a thin lens fixed in the $z = 0$ plane, propagating along the positive z-axis. The system's transfer matrix is expressed as:

$$\begin{bmatrix} A & B \\ C & D \end{bmatrix} = \begin{bmatrix} 1 - \frac{z}{f} & z \\ -\frac{1}{f} & 1 \end{bmatrix}, \tag{7}$$

where f represents the focal length.

The CSD function of a TCGSMA beam propagating through the $ABCD$ optical system can be treated by the Collins formula [39]:

$$W(\boldsymbol{\rho}_1, \boldsymbol{\rho}_2, z) = \frac{k^2}{4\pi^2 B^2}\iint p(\boldsymbol{v}) H^*(\boldsymbol{\rho_1'}, \boldsymbol{v}, z) H(\boldsymbol{\rho_2'}, \boldsymbol{v}, z)\mathrm{d}^2\boldsymbol{v}, \tag{8}$$

where

$$H(\boldsymbol{\rho}, \boldsymbol{v}, z) = \iint H(\boldsymbol{\rho}', \boldsymbol{v}) \exp\left\{\frac{ik}{2B}[A(x^2 + y^2) - 2(xx' + yy') + D(x'^2 + y'^2)]\right\}\mathrm{d}^2\boldsymbol{\rho}'. \tag{9}$$

By substituting Equations (3) and (7) into Equation (8), the CSD function of a TMCGSM array on propagation can be given by the formula:

$$\begin{aligned} W(\boldsymbol{\rho}_1, \boldsymbol{\rho}_2, z) = \; & \frac{k^2}{4B^2\Omega}\exp\left[\frac{ikD(x_2^2 + y_2^2 - x_1^2 - y_1^2)}{2B}\right] \\ & \times \exp\left[-\frac{k^2}{4B^2}\left(\frac{x_2^2}{\xi_{x2}} + \frac{y_2^2}{\xi_{y2}} + \frac{x_1^2}{\xi_{x1}} + \frac{y_1^2}{\xi_{y1}}\right)\right] \\ & \times \iint G(v_x, v_y) p(v_x, v_y)\mathrm{d}v_x\mathrm{d}v_y, \end{aligned} \tag{10}$$

where

$$G(v_x, v_y) = \exp\left(-\alpha_x v_x^2 - \alpha_y v_y^2 + \beta_x v_x + \beta_y v_y + \xi v_x v_y\right), \tag{11}$$

$$\xi_{x1} = {\xi_{x2}}^* = \frac{1}{2\sigma_x^2} + \frac{ikA}{2B}, \xi_{y1} = {\xi_{y2}}^* = \frac{1}{2\sigma_y^2} + \frac{ikA}{2B}, \tag{12}$$

$$\Omega^2 = \xi_{x1}\xi_{x2}\xi_{y1}\xi_{y2}, \xi = \frac{iu}{2}\left(\frac{1}{\xi_{x1}} - \frac{1}{\xi_{x2}}\right) + \frac{iu}{2}\left(\frac{1}{\xi_{y2}} - \frac{1}{\xi_{y1}}\right), \tag{13}$$

$$\alpha_x = \frac{1}{4}\left(\frac{1}{\xi_{x1}} + \frac{1}{\xi_{x2}}\right) - \frac{u^2}{4}\left(\frac{1}{\xi_{y1}} + \frac{1}{\xi_{y2}}\right), \alpha_y = \frac{1}{4}\left(\frac{1}{\xi_{y1}} + \frac{1}{\xi_{y2}}\right) - \frac{u^2}{4}\left(\frac{1}{\xi_{x1}} + \frac{1}{\xi_{x2}}\right), \tag{14}$$

$$\beta_x = -\frac{k}{2B}\left(\frac{x_1}{\xi_{x1}} + \frac{x_2}{\xi_{x2}}\right) + \frac{iku}{2B}\left(\frac{y_2}{\xi_{y2}} - \frac{y_1}{\xi_{y1}}\right), \beta_y = -\frac{k}{2B}\left(\frac{y_1}{\xi_{y1}} + \frac{y_2}{\xi_{y2}}\right) + \frac{iku}{2B}\left(\frac{x_1}{\xi_{x1}} - \frac{x_2}{\xi_{x2}}\right), \tag{15}$$

By substituting Equation (4) into Equation (10) and performing the integral, we obtain the following formula for the CSD:

$$\begin{aligned} W(\boldsymbol{\rho}_1, \boldsymbol{\rho}_2, z) = \; & \frac{\pi k^2 \delta_x \delta_y}{8B^2 NM\Omega} \exp\left[\frac{ikD}{2B}\left({\boldsymbol{\rho}_2}^2 - {\boldsymbol{\rho}_1}^2\right)\right] \\ & \times \exp\left[-\frac{k^2}{4B^2}\left(\frac{{x_1}^2}{\xi_{x1}} + \frac{{y_1}^2}{\xi_{y1}} + \frac{{x_2}^2}{\xi_{x2}} + \frac{{y_2}^2}{\xi_{y2}}\right)\right] \\ & \times \int \sum_{n=-P}^{P} \Gamma[\Phi_+ + \Phi_-] \exp\left(-2\pi^2 n^2 R_x^2\right) \\ & \times \sum_{m=-Q}^{Q} \Delta[\Theta_+ + \Theta_-] \exp\left(-2\pi^2 m^2 R_y^2\right) \mathrm{d}v_y, \end{aligned} \tag{16}$$

where

$$\Phi_\pm = \exp\left[\frac{\left(\pm 4\pi^2 \delta_x n R_x + \beta_x + \xi v_y\right)^2}{4(2\pi^2\delta_x^2 + \alpha_x)}\right], \Theta_\pm = \exp\left(\pm 4\pi^2 \delta_y m R_y v_y\right), \tag{17}$$

$$\Gamma = \sqrt{\frac{\pi}{2\pi^2\delta_x^2 + \alpha_x}}, \Delta = \exp\left(-2\pi^2\delta_y^2 v_y^2 - \alpha_y v_y^2 + \beta_y v_y\right). \tag{18}$$

The spectral density can be obtained by the equation $S(\boldsymbol{\rho}, z) = W(\boldsymbol{\rho}, \boldsymbol{\rho}, z)$ with $\boldsymbol{\rho}_1 = \boldsymbol{\rho}_2 = \boldsymbol{\rho}$. The degree of coherence (DOC) between a pair of points is presented in the following equation: [40]

$$\mu(\boldsymbol{\rho}_1, \boldsymbol{\rho}_2, z) = \frac{W(\boldsymbol{\rho}_1, \boldsymbol{\rho}_2, z)}{\sqrt{S(\boldsymbol{\rho}_1, \boldsymbol{\rho}_1, z)}\sqrt{S(\boldsymbol{\rho}_2, \boldsymbol{\rho}_2, z)}}. \tag{19}$$

3. Numerical Examples

In this section, we present a numerical analysis of the typical properties of a focused TMCGSM array during propagation. The focal length and wavelength are chosen as f= 400 mm and λ= 632 nm, respectively. Figure 1 displays the evolution of the normalized spectral density and the spectral DOC of the focused twisted field. Due to the presence of a multi-cosine correlation structure, the field gradually turns its primitive Gaussian beam shape into a $M \times N$ array profile along the propagation axis. Meanwhile, the twist terms not only allow the entire intensity profile to rotate clockwise by 90 degrees, but also induce a non-uniform distribution of the lattice. Specifically, the intensity of the elements near the propagation axis would be attenuated due to the contribution of twist. It is seen from row 2 that the DOC also exhibits a weak twist effect, and as the propagation distance increases, the coherence profile rotates clockwise around the beam center and transforms from a lattice-like distribution to an elliptical Gaussian shape.

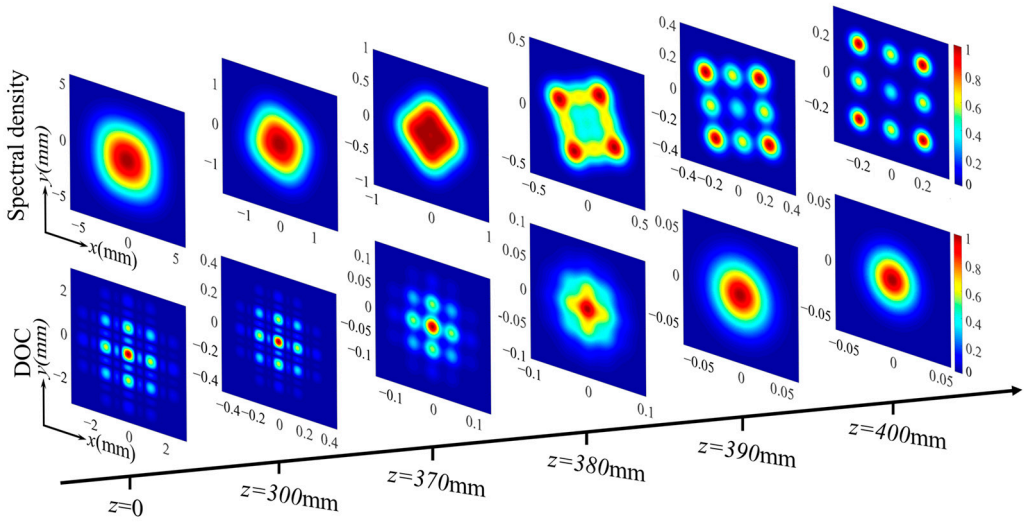


Figure 1. Normalized spectral density and DOC generated by a focused TMCGSM source at several propagation distances. The parameters of the source are set as $u = 0.05$, $\delta_x = \delta_y = 0.2$ mm, $\sigma_x = \sigma_y = 2$ mm, $R_x = R_y = 1$ and $M = N = 3$.

Figure 2 shows the influence of the twist factor on the spectral density in the focal plane. With the choice of $u = 0$, a lattice field with identical Gaussian-like lobes appears in the focal plane as expected. With the addition of u, a spectral density attenuation in the central area would be observed. It is worth mentioning that the intensity declines more rapidly with the increase in twist strength. If the twist effect is strong enough, the central lobes vanish. Such a controllable non-uniform array distribution, which possesses great potential in multi-particle trapping, was not previously observed.

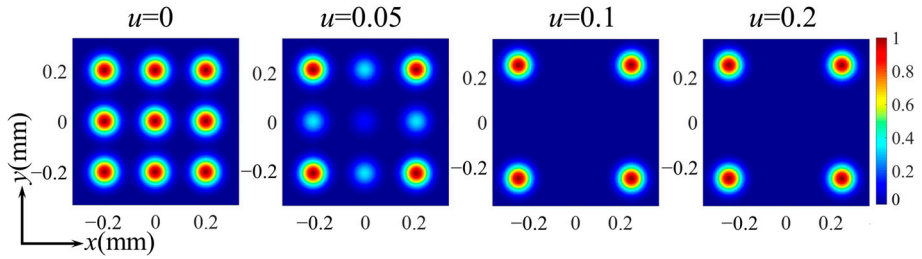


Figure 2. Normalized spectral density in the focal plane with various twist factors. The relevant parameters set here are the same as in Figure 1.

Figure 3 shows the evolution behavior of the spectral density with the various coherence factor R_i. For an isotropic correlated case with $R_x = R_y$ (seen in row 1), the beam patterns in the two orthogonal directions are the same. Otherwise, the intensity spot in the two directions will evolve with different behaviors, as shown in row 2 and row 3. By comparing these figures, one sees that with a smaller R_i, the field can be more resistant to the attenuation induced by the twist. Moreover, the anisotropic of the source coherence distribution induces an asymmetrical intensity profile, which could be explained by the reciprocity theorem. Figure 4 illustrates the modulation effect of relevant parameters on the far-zone intensity profiles. It is revealed that the contour of the array is mainly determined by the summation indexes M and N. while the local distribution near the propagation axis is jointly modulated by the coherence width and the source length. Further, the splitting tendency could be depressed by a larger δ_i or a smaller σ_i.

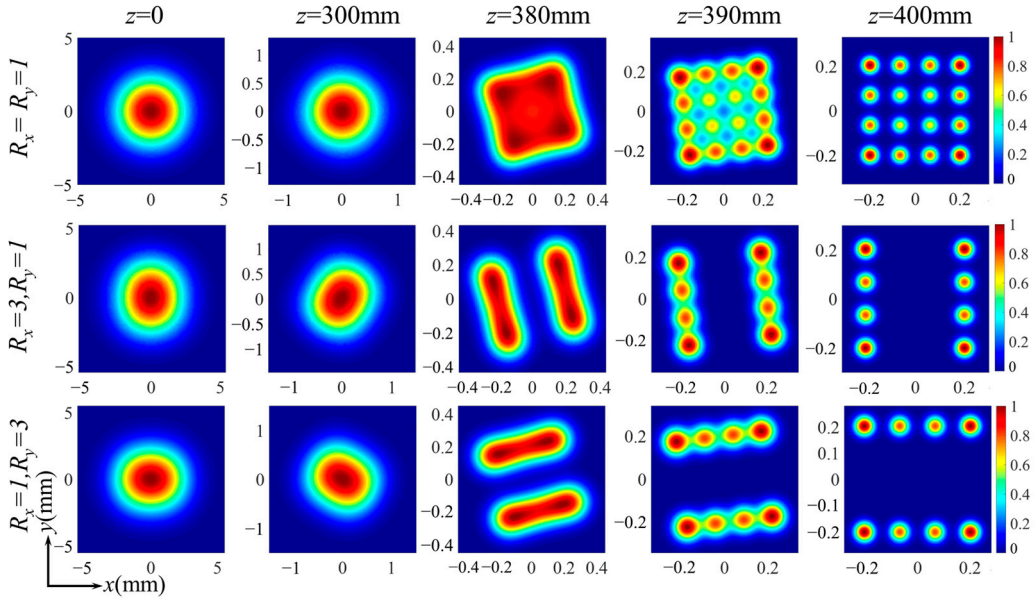


Figure 3. Evolution behavior of the normalized spectral density with different coherence factors. The other parameters are set as $u = 0.05$, $\delta_x = \delta_y = 0.3$ mm, $\sigma_x = \sigma_y = 2$ mm and $M = N = 4$.

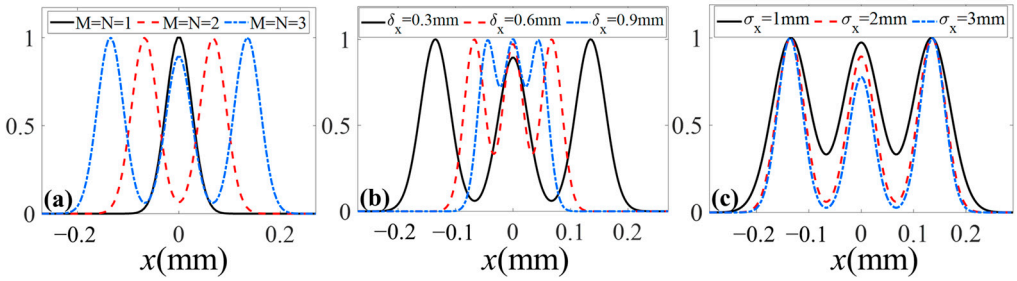


Figure 4. Normalized spectral density of a TMCGSM array with $u = 0.05$ in the focal plane for different variables. (**a**) $\delta_x = 0.3$mm, $\sigma_x = 2$ mm. (**b**) $\sigma_x = 2$ mm, $M = N = 3$. (**c**) $\delta_x = 2$ mm, $M = N = 3$.

Figure 5 presents the evolution of the DOC $\mu(\boldsymbol{\rho}_1, \boldsymbol{\rho}_2, z)$ between two symmetrical points for an isotropic correlated field (seen in row 1) and non-isotropic correlated cases (seen in row 2 and row 3). It is revealed that all of the coherence images rotate clockwise along the propagation axis, which is similar to those of the spectral density shown in Figure 3. By comparing row 1 with the others, one finds that the twist effect is more obvious with a non-isotropic correlated source. This implies that the twist effect can be enhanced by the non-isotropic correlation factor of the source. Specifically, the greater the difference of correlation factor, the more visible the twist. As can be seen from row 2 and row 3, a larger R_i will degenerate the DOC more rapidly. The DOC presents a vertical ellipse with $R_x > R_y$, while it presents a horizontal ellipse with $R_x < R_y$. The dependence of the spectral DOC on the twist factor, the coherence width and the source length has been presented in Figure 6. It is revealed from Figure 6a that with the increase in twist strength, the coherence distribution narrows down. It is also seen from Figure 6b,c that the coherence drops more efficiently with a smaller δ_i or a larger σ_i.

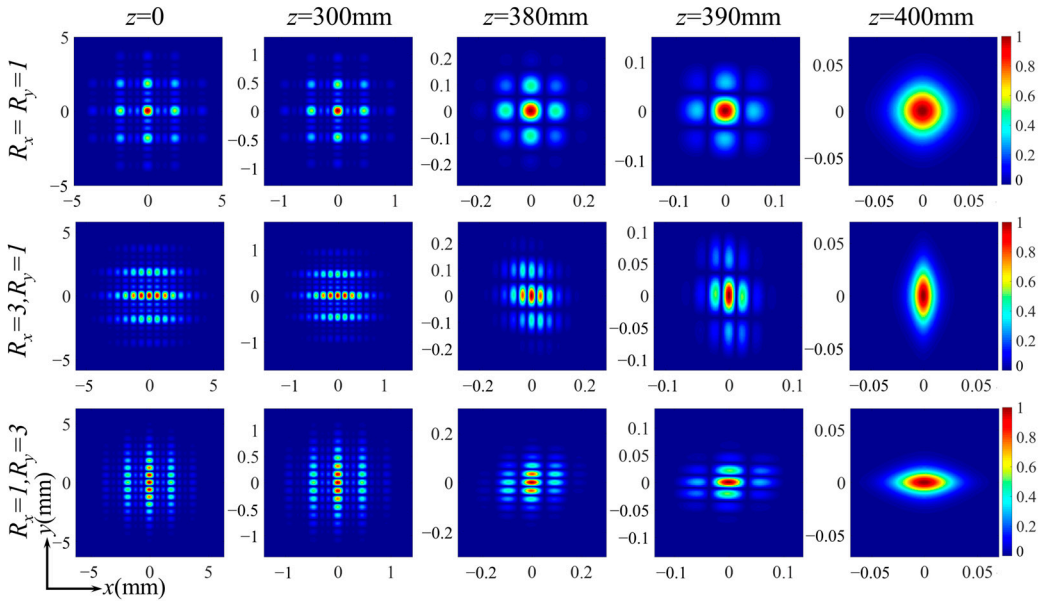


Figure 5. Spectral DOC $\mu(\boldsymbol{\rho}_1, \boldsymbol{\rho}_2, z)$ between a pair of points $\boldsymbol{\rho}_1 = (x/2, y/2)$ and $\boldsymbol{\rho}_2 = (-x/2, -y/2)$ at several propagation distances. The relevant parameters set here are the same as in Figure 3.

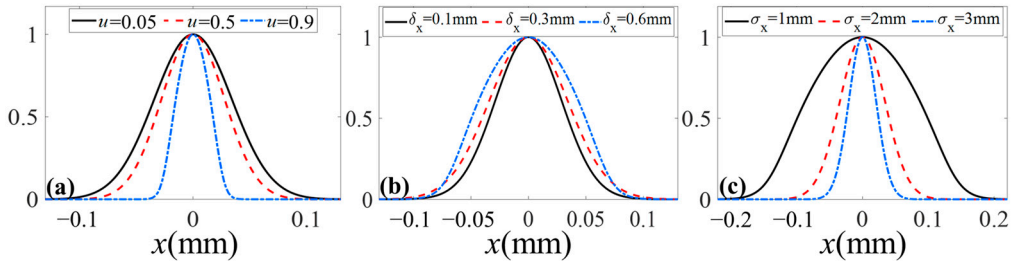


Figure 6. DOC $\mu(\boldsymbol{\rho}_1, \boldsymbol{\rho}_2, z)$ in the focal plane for different variables. (**a**) $\delta_x = 0.3$ mm, $\sigma_x = 2$ mm, $M = N = 3$. (**b**) $\sigma_x = 2$ mm, $u = 0.05$, $M = N = 3$. (**c**) $\delta_x = 0.3$ mm, $u = 0.05$, $M = N = 3$.

4. Discussion

Most of the previous twisted array beams are devised by mapping the twist phase to untwisted array twisted CSD functions, such as twisted GSMAs [9], and twisted ring-shaped GSMAs [36]. Although they have different array profiles, the twist phase leads to the fact that they all have the same twist patterns, that is, each element rotates about its own lobe center. The twist has a more complicated form in the TMCGSM arrays proposed in our work; specifically, the twist factor exists in the correlation function instead of as a simple phase. As a result, the intensity profile twists about the axis as a whole. Additionally, due to the contribution of the twisted correlation in the CSD, the field can produce a non-uniform array distribution, which is quite distinct from twisted GSMAs. Although most twisted lattice fields present identical element lobes, an exception is the twisted sinc-correlation Schell-model array introduced in Ref. [37], which can present a non-uniform array distribution. While the twisted sinc-correlation Schell-model array presents non-average lobes with different profiles and different intensities, our model shows Gaussian-like lobes with a controllable intensity. Such novel features make the TMCGSM arrays more capable of manipulation in practical application.

The TMCGSM array can be experimentally realized by using a general method described in [20], by implementing the continuous coherent beam integral function in a discrete form. Firstly, the pseudo-modes of the source can be calculated according to Equation (16). Secondly, a phase-programmable SLM displays a phase hologram to generate the coherence pattern of the model. Then, an amplitude SLM can be used to generate anisotropic beams. Finally, a CCD camera is used to record the intensity.

5. Summary

We have presented a novel twisted partially coherent array in which the correlation structure is described by a twisted multi-cosine Gaussian Shell-model function, named the TMCGSM array. The spectral density and the spectral DOC of a focused TMCGSM array beam propagating in vacuum have been studied. Unlike most twisted lattice fields that present identical element lobes, our model could produce a non-uniform array distribution in the focal plane, and the intensity pattern of the central lobes could be controlled by the twist strength. Moreover, due to the novel twisted correlation, the array profile rotates around the propagation axis, which is an unusual rotation mode compared to other twisted arrays. The features of the field, including the lattice dimension and the intensity of lobes, could be properly modulated by varying the source parameters. We also revealed that an obvious twist effect could be observed in the coherence curves under certain conditions. This novel twisted non-uniform array beam could provide potential applications in dynamic multi-particle trapping.

Author Contributions: Conceptualization, M.T.; data curation, S.D. and Y.Z.; methodology, P.Y.; project administration, M.T. and X.L.; software, S.D. and Y.Y.; supervision, X.L.; writing—original draft, M.T. and S.D.; writing—review and editing, X.L. All authors have read and agreed to the published version of the manuscript.

Funding: This research was funded by the National Natural Science Foundation of China (No. 12174089), the Natural Science Foundation of Henan Province (Nos. 222300420042, 242300420635), and the Cultivation Program for Young Backbone Teachers of Higher Education Institutions in Henan Province (No. 2023GGJS047).

Institutional Review Board Statement: Not applicable.

Informed Consent Statement: Not applicable.

Data Availability Statement: Data are contained within the article.

Conflicts of Interest: The authors declare no conflicts of interest.

References

1. Korotkova, O. *Random Beams: Theory and Applications*; CRC Press: Boca Raton, FL, USA, 2013.
2. Kato, Y.; Mima, K.; Miyanaga, N.; Arinaga, S.; Kitagawa, Y.; Nakatsuka, M.; Yamanaka, A.C. Random phasing of high-power lasers for uniform target acceleration and plasma-instability suppression. *Phys. Rev. Lett.* **1984**, *53*, 1057–1060. [CrossRef]
3. Ferri, F.; Magatti, D.; Gatti, A.; Bache, M.; Brambilla, E.; Lugiato, L.A. High-resolution ghost image and ghost diffraction experiments with thermal light. *Phys. Rev. Lett.* **2005**, *94*, 183602. [CrossRef] [PubMed]
4. Auñón, J.M.; Nieto-Vesperinas, M. Partially coherent fluctuating sources that produce the same optical force as a laser beam. *Opt. Lett.* **2013**, *38*, 2869–2872. [CrossRef] [PubMed]
5. Zhang, J.F.; Wang, Z.Y.; Cheng, B.; Wang, Q.Y.; Wu, B.; Shen, X.X.; Lin, Q. Atom cooling by partially spatially coherent lasers. *Phys. Rev. A* **2013**, *88*, 023416. [CrossRef]
6. Wu, G.; Cai, Y. Detection of a semirough target in turbulent atmosphere by a partially coherent beam. *Opt. Lett.* **2011**, *36*, 1939–1941. [CrossRef]
7. Liu, Y.; Zhang, X.; Dong, Z.; Peng, D.; Chen, Y.; Wang, F.; Cai, Y. Robust Far-Field Optical Image Transmission with Structured Random Light Beams. *Phys. Rev. Appl.* **2022**, *17*, 024043. [CrossRef]
8. Peng, D.; Huang, Z.; Liu, Y.; Chen, Y.; Wang, F.; Ponomarenko, S.A.; Cai, Y. Optical coherence encryption with structured random light. *PhotoniX* **2021**, *2*, 6. [CrossRef]
9. Simon, R.; Mukunda, N. Twisted Gaussian Schell-model beams. *J. Opt. Soc. Am. A* **1993**, *10*, 95–109. [CrossRef]
10. Friberg, A.T.; Tervonen, E.; Turunen, J. Interpretation and experimental demonstration of twisted Gaussian Schell-model beams. *J. Opt. Soc. Am. A* **1994**, *11*, 1818–1826. [CrossRef]
11. Wang, F.; Cai, Y.; Eyyuboğlu, H.T.; Baykal, Y. Twist phase-induced reduction in scintillation of a partially coherent beam in turbulent atmosphere. *Opt. Lett.* **2012**, *37*, 184–186. [CrossRef]
12. Tong, Z.; Korotkova, O. Beyond the classical Rayleigh limit with twisted light. *Opt. Lett.* **2012**, *37*, 2595–2597. [CrossRef] [PubMed]
13. Cai, Y.; Zhu, S. Orbital angular moment of a partially coherent beam propagating through an astigmatic ABCD optical system with loss or gain. *Opt. Lett.* **2014**, *39*, 1968–1971. [CrossRef] [PubMed]
14. Wu, G. Propagation properties of a radially polarized partially coherent twisted beam in free space. *J. Opt. Soc. Am. A* **2016**, *33*, 345–350. [CrossRef]
15. Zhang, Y.; Yan, H.; Zhao, D. Optical trapping Rayleigh particles with a twist effect. *Opt. Laser Eng.* **2020**, *130*, 106101. [CrossRef]

16. Borghi, R.; Gori, F.; Guattari, G.; Santarsiero, M. Twisted Schell-model beams with axial symmetry. *Opt. Lett.* **2015**, *40*, 4504–4507. [CrossRef] [PubMed]
17. Gori, F.; Santarsiero, M. Devising genuine twisted cross-spectral densities. *Opt. Lett.* **2018**, *43*, 595–598. [CrossRef]
18. Mei, Z.; Korotkova, O. Random sources for rotating spectral densities. *Opt. Lett.* **2017**, *42*, 255–258. [CrossRef]
19. Mei, Z.; Korotkova, O. Twisted EM beams with structured correlations. *Opt. Lett.* **2018**, *43*, 3905–3908. [CrossRef]
20. Tian, C.; Zhu, S.; Huang, H.; Cai, Y.; Li, Z. Customizing twisted Schell-model beams. *Opt. Lett.* **2020**, *45*, 5880–5883. [CrossRef]
21. Xia, Y.; Wang, H.; Liu, L.; Chen, Y.; Wang, F.; Cai, Y. Experimental Synthesis and Demonstration of the Twisted Laguerre–Gaussian Schell-Mode Beam. *Photonics* **2023**, *10*, 314. [CrossRef]
22. Zhou, Y.; Cui, Z.; Han, Y. Polarization and coherence properties in self-healing propagation of a partially coherent radially polarized twisted beam. *Opt. Express* **2022**, *30*, 23448–23462. [CrossRef] [PubMed]
23. Yang, Y.; Wu, Y.; Zheng, X.; Shi, J.; Luo, Y.; Huang, J.; Deng, D. Particle manipulation with twisted circle Pearcey vortex beams. *Opt. Lett.* **2023**, *48*, 3535–3538. [CrossRef] [PubMed]
24. Fu, G.; Chen, J.; Qi, G.; Wu, Y.; Zhang, X.; Wang, H.; Shi, Y.; Zhao, C.; Jin, S. Generating a hollow twisted correlated beam using correlated perturbations. *Opt. Express* **2023**, *31*, 1442–1451. [CrossRef]
25. Hu, J.; Wei, W.; Sun, Z.; Li, X.; Qian, Y. Customizing twisted structured light beams. *Opt. Laser Technol.* **2025**, *181*, 111708. [CrossRef]
26. Anderson, B.P.; Gustavson, T.L.; Kasevich, M.A. Atom trapping in nondissipative optical lattices. *Phys. Rev. A* **1996**, *53*, R3727–R3730. [CrossRef] [PubMed]
27. MacDonald, M.P.; Paterson, L.; Volke-Sepulveda, K.; Arlt, J.; Sibbet, W.; Dholakia, K. Creation and manipulation of three-dimensional optically trapped structures. *Science* **2002**, *296*, 1101–1103. [CrossRef]
28. MacDonald, M.; Spalding, G.; Dholakia, K. Microfluidic sorting in an optical lattice. *Nature* **2003**, *426*, 421–424. [CrossRef]
29. Mei, Z.; Zhao, D.; Korotkova, O.; Mao, Y. Gaussian Schell-model arrays. *Opt. Lett.* **2015**, *40*, 5662–5665. [CrossRef]
30. Ding, Y.; Zhao, D. Random medium model for producing optical coherence lattice. *Opt. Express* **2017**, *25*, 25222–25233. [CrossRef]
31. Mao, Y.; Mei, Z. Random sources generating ring-shaped optical lattice. *Opt. Commun.* **2016**, *381*, 222–226. [CrossRef]
32. Wan, L.; Zhao, D. Optical coherence grids and their propagation characteristics. *Opt. Express* **2018**, *26*, 2168–2180. [CrossRef] [PubMed]
33. Wan, L.; Zhao, D. Twisted Gaussian Schell-model array beams. *Opt. Lett.* **2018**, *43*, 3554–3557. [CrossRef] [PubMed]
34. Zhou, Y.; Zhao, D. Statistical properties of electromagnetic twisted Gaussian Schell-model array beams during propagation. *Opt. Express* **2019**, *27*, 19624–19632. [CrossRef] [PubMed]
35. Wang, J.; Huang, H.; Chen, Y.; Wang, H.; Zhu, S.; Li, Z.; Cai, Y. Twisted partially coherent array sources and their transmission in anisotropic turbulence. *Opt. Express* **2018**, *26*, 25974–25988. [CrossRef] [PubMed]
36. Zheng, S.; Yuan, C.; Ji, X.; Wang, T. Ring-shaped twisted Gaussian Schell-model array beams. *J. Opt. Soc. Am. A* **2020**, *37*, 444–449. [CrossRef]
37. Zhou, Y.; Tang, M.; Li, H.; Li, X. Twisted sinc-correlation Schell-model array beams. *Opt. Express* **2023**, *31*, 26069–26077. [CrossRef]
38. Gori, F.; Santarsiero, M. Devising genuine spatial correlation functions. *Opt. Lett.* **2007**, *32*, 3531–3533. [CrossRef]
39. Gbur, G. *Singular Optics*; CRC Press: Boca Raton, FL, USA, 2017.
40. Mandel, L.; Wolf, E. *Coherence and Quantum Optics*; Springer: Boston, MA, USA, 1973.

Disclaimer/Publisher's Note: The statements, opinions and data contained in all publications are solely those of the individual author(s) and contributor(s) and not of MDPI and/or the editor(s). MDPI and/or the editor(s) disclaim responsibility for any injury to people or property resulting from any ideas, methods, instructions or products referred to in the content.